Published in final edited form as:
Nature. 2014 July 10; 511(7508): 184–190. doi:10.1038/nature13323.

Aryl hydrocarbon receptor control of a disease tolerance defense pathway

Alban Bessede[1,2,17], **Marco Gargaro**[1,17], **Maria T Pallotta**[1], **Davide Matino**[1], **Giuseppe Servillo**[3], **Cinzia Brunacci**[3], **Silvio Bicciato**[4], **Emilia MC Mazza**[4], **Antonio Macchiarulo**[5], **Carmine Vacca**[1], **Rossana Iannitti**[1], **Luciana Tissi**[1], **Claudia Volpi**[1], **Maria L Belladonna**[1], **Ciriana Orabona**[1], **Roberta Bianchi**[1], **Tobias Lanz**[6,7], **Michael Platten**[6,7], **Maria A Della Fazia**[3], **Danilo Piobbico**[3], **Teresa Zelante**[1], **Hiroshi Funakoshi**[8], **Toshikazu Nakamura**[9], **David Gilot**[10], **Michael S Denison**[11], **Gilles J Guillemin**[12], **James B DuHadaway**[13], **George C Prendergast**[13], **Richard Metz**[14], **Michel Geffard**[2], **Louis Boon**[15], **Matteo Pirro**[16], **Alfonso Iorio**[17], **Bernard Veyret**[2], **Luigina Romani**[1], **Ursula Grohmann**[1], **Francesca Fallarino**[1,18], and **Paolo Puccetti**[1,18]

[1]Department of Experimental Medicine, University of Perugia, Perugia, Italy [2]University of Bordeaux, IMS Laboratory, Pessac, France [3]Department of Clinical and Experimental Medicine, University of Perugia, Italy [4]Center for Genome Research, Department of Life Sciences, University of Modena and Reggio Emilia, Modena, Italy [5]Department of Chemistry and Technology of Drugs, University of Perugia, Italy [6]Experimental Neuroimmunology Unit, German Cancer Research Center, Heidelberg, Germany [7]Department of Neurooncology, University Hospital, Heidelberg, Germany [8]Center for Advanced Research and Education, Asahikawa Medical University, Asahikawa, Japan [9]Kringle Pharma Joint Research Division for Regenerative Drug Discovery, Center for Advanced Science and Innovation, Osaka University, Osaka, Japan [10]4CNRS UMR 6290, Université de Rennes, Rennes, France [11]Department of Environmental Toxicology, University of California, Davis, CA [12]Australian School of Advanced Medicine (ASAM), Macquarie University, NSW, 2109, Australia [13]Lankenau Institute for Medical Research, Wynnewood, PA [14]New Link Genetics Corporation, Ames, IA [15]Bioceros, Utrecht, The Netherlands [16]Department of Clinical and Experimental Medicine, University of Perugia, Italy [17]Clinical Epidemiology and Biostatistics and Medicine, McMaster University, Canada

Abstract

[18]These authors share senior authorship on this paper; to whom correspondence should be addressed (P.P., plopcc@tin.it; F.F., fllfnc@tin.it).
[17]These authors contributed equally to this work

Author Contributions

A.B. and M.G. designed and conducted all experiments unless otherwise indicated below; M.T.P., D.M., and C.V. analyzed IDO and Src phosphorylation; S.B., E.M.C.M., D.P., M.P., and A.I. conducted bioinformatics studies and statistical analysis. A.M. performed homology modeling and docking studies. R.I., T.Z., M.A.D.F., L.R., and L.T. conducted the *in vivo* studies with *Salmonella* and GBS. C.V., M.L.B., C.O., G.S., C.B., and R.B. contributed to specific experimental designs; T.L., M.P., H.F., and T.N. made possible, and designed, the experiments with TDO2-deficient mice; J.B.D., G.C.P., and R.M. made possible, and designed, the experiments with IDO2-deficient mice; D.G., M.S.D., G.J.G., M.G., B.V., L.B. and U.G. provided conceptual help and precious reagents throughout experimentation; F.F. designed and supervised all experiments; P.P. supervised the overall study and wrote the manuscript.

Competing Financial Interests

The authors declare no competing financial interests.

Summary—Disease tolerance is the ability of the host to reduce the impact of infection on host fitness. Analysis of disease tolerance pathways could provide new approaches for treating infections and other inflammatory diseases. Typically, an initial exposure to bacterial lipopolysaccharide (LPS) induces a state of refractoriness to further LPS challenge ("endotoxin tolerance"). We found that a first exposure to LPS activated the ligand-operated transcription factor aryl hydrocarbon receptor (AhR) and the hepatic enzyme tryptophan 2,3-dioxygenase 2, which provided an activating ligand to the former, to downregulate early inflammatory gene expression. However, on LPS rechallenge, AhR engaged in long-term regulation of systemic inflammation only in the presence of indoleamine 2,3-dioxygenase 1 (IDO1). AhR complex-associated Src kinase activity promoted IDO1 phosphorylation and signaling ability. The resulting endotoxin-tolerant state was found to protect mice against immunopathology in gram-negative and gram-positive infections, pointing to a role for AhR in contributing to host fitness.

Introduction

Although lipopolysaccharide (LPS)-induced proinflammatory molecules are indispensable for counteracting the growth and dissemination of gram-negative bacteria, overproduction can lead to sepsis syndrome, also known as endotoxin shock. However, a prior exposure to a low level of LPS induces a durable state of cell refractoriness to subsequent LPS challenge, a condition known as endotoxin tolerance[1-4]. The complex events underlying this phenomenon remain poorly understood, despite a recent resurgence of interest in this effect, which involves multiple downstream effector cells and mechanisms. Endotoxin tolerance, not merely amounting to a shutdown of LPS-induced responses, involves reprogramming of gene expression[5] and chromatin remodeling[6]. The occurrence of endotoxin tolerance has been reported in several disease settings, including sepsis, trauma, surgery, and pancreatitis, underlining its clinical significance. Pharmacologic modulation of LPS-responsive genes to accelerate the onset of endotoxin tolerance would be beneficial in clinical settings dominated by acute hyperinflammatory responses to infection[5]. In addition, endotoxin derived from gram-negative bacteria is known to have immunomodulatory and allergy-protective potential[7].

In experimental models, the aryl hydrocarbon receptor (AhR), a ligand-operated transcription factor[8,9], participates in the transcriptional regulation of several LPS-responsive genes, and AhR-deficient mice are more sensitive to endotoxin shock than wild-type (WT) mice[10]. This suggests a crucial function of AhR in modulating the inflammatory response mediated by LPS and Toll-like receptor (TLR)4 signaling[5]. Yet, the nature of the endogenous ligands that drive AhR-regulated gene expression in response to TLR4 activation has been unclear[11]. Also, the potential role of AhR in endotoxin tolerance has never been addressed experimentally.

The first step in tryptophan catabolism is the cleavage of the 2,3-double bond of the indole ring of tryptophan[12]. In mammals, this reaction is performed independently by indoleamine 2,3-dioxygenase 1 (IDO1), tryptophan 2,3-dioxygenase 2 (TDO2; mostly expressed in the liver), and the recently discovered indoleamine 2,3-dioxygenase 2 (IDO2; a paralogue of IDO1). When induced by proinflammatory cytokines[13], tryptophan degradation by IDO1 yields a series of catabolites – collectively known as kynurenines[14] – that regulate immune

homeostasis by acting as AhR ligands and allowing the generation of regulatory T cells[15-17], which protect mice from chronic hyperinflammatory responses[18]. Increased plasma kynurenine levels and kynurenine-to-tryptophan ratios have been found in patients with systemic inflammatory response syndrome, sepsis, and septic shock, but the biological significance and prognostic value of these findings have remained uncertain[19].

In the current study we used C57BL/6 WT, AhR-deficient mice, and mice lacking IDO1, IDO2, or TDO2 to investigate the role of AhR and tryptophan catabolism in primary LPS responsiveness and in the induction of endotoxin tolerance. We found that overreacting responses to primary LPS challenge were mitigated by AhR and TDO2-dependent tryptophan catabolism. Endotoxin tolerance, in contrast, required the combined effects of AhR, IDO1, and the cytokine transforming growth factor-β (TGF-β). The protective, LPS-triggered tolerant state was not restricted to LPS- or gram-negative bacteria–induced immunopathology, in that it also specifically targeted inflammatory cytokine production in a *Streptococcus*-induced multifocal septic arthritis model.

Results

Ahr$^{-/-}$ and *Tdo2* $^{-/-}$ mice show increased susceptibility to primary endotoxemia

During sepsis, activation of phagocytes leads to tissue damage by migratory neutrophils and overproduction of proinflammatory cytokines, which worsen systemic inflammation and result in hemodynamic changes, multiple organ failure, and ultimately death. Synthesis of acute phase proteins occurs in the liver. We investigated the effects of a first, sublethal dose (10 mg/kg, i.p.) of LPS in C57BL/6 WT, *Ido1*$^{-/-}$, *Ido2*$^{-/-}$, *Tdo2*$^{-/-}$, and *Ahr*$^{-/-}$ mice (Fig. 1a). Susceptibility to endotoxemia was greatly increased in AhR knockout (KO) and TDO2 KO mice with respect to WT controls, with limited (IDO1) or no (IDO2) effects of either indoleamine 2,3-dioxygenase deficiency. LPS induced an increase in serum kynurenine-to-tryptophan (kyn/trp) ratios, an effect that was selectively negated by *Tdo2* deficiency (Fig. 1b).

Mice of the different genotypes were challenged with a wide range (2.5–80 mg/kg) of LPS doses, to calculate the median lethal dose (LD_{50}) of endotoxin (Fig. 1c). LD_{50} values (mg/kg) varied among the different genotypes, being highest in WT (27.3), *Ido1*$^{-/-}$ (22.5) and *Ido2*$^{-/-}$ (32.1) mice, and considerably lower in *Tdo2*$^{-/-}$ (9.7) and *Ahr*$^{-/-}$ (5.2) mice. Consistent results were obtained using either the IDO1 and IDO2 inhibitor 1-methyltryptophan (1-MT) or the TDO2-selective inhibitor 680C91 (Extended Data Fig. 1a). LD_{50} values varied between inhibitor-treated mice, being considerably higher in 1-MT–treated (22.8) than 680C91-treated (7.2) mice (Extended Data Fig. 1b). Histopathology of the lungs (Fig. 1d) and liver (Fig. 1e) revealed that inflammation and neutrophil infiltration were most intense in AhR KO and TDO2 KO mice. This suggested that, upon primary LPS challenge, IDO1 and IDO2 may not contribute significantly to protection[20] and that AhR and hepatic TDO2 are, in contrast, functionally important for protection.

Analysis of blood samples from WT, *Ahr*$^{-/-}$, *Ido1*$^{-/-}$, or *Tdo2*$^{-/-}$ mice, at different times of LPS administration (10 mg/kg), showed a marked increase in plasma concentrations of TNF-α and IL-6, (peaking at 2 h under all conditions, and only marginally declining

thereafter in *Ahr*$^{-/-}$ and *Tdo2*$^{-/-}$mice), IL-1β (peak levels at 6 h, further increasing at 24 h in *Ahr*$^{-/-}$ and *Tdo2*$^{-/-}$ mice), and IL-10 (with high, sustained production only in WT and *Ido1*$^{-/-}$ mice) (Fig. 1f). Thus, in accordance with previous data in the literature, resistance to primary LPS challenge correlated with an early (2–6 h), yet reversible (24 h), increase in plasma levels of TNF-α, IL- 6, IL-1β – all dysregulated by AhR deficiency[10,21,22] – and with a progressive increase in IL-10, (in WT and *Ido1*$^{-/-}$ mice, as opposed to the stationary levels in *Ahr*$^{-/-}$ and *Tdo2*$^{-/-}$ mice). The AhR- and TDO2-dependent induction of IL-10 was crucial in regulating the proinflammatory response to endotoxin in WT mice (Extended Data Fig. 2a,b). Exogenous IL-10 (250 ng/mouse, daily, administered from challenge through day 5) significantly improved survival in both TDO2- and AhR-deficient mice receiving 10 mg/kg LPS on day 0 (Extended Data Fig. 2c). TGF-β was not detectable under any conditions over the timeframe of observation.

Real-Time PCR analysis revealed that, in response to 10 mg/kg LPS, AhR was expressed early (24 h) at the injection site, in peritoneal exudate cells (PECs). No modulation was observed in the liver. *Tdo2* was induced in the liver at 6–24 h of LPS injection, whereas no induction was observed in PECs (Fig. 1g). Also, no induction at all of *Ahr* and *Tdo2* occurred in *Tlr4*$^{-/-}$ mice. Protein expressions of AhR, TDO2, IDO1 and IDO2 were assessed at 24 h, by immunoblot analysis in PECs and liver cells, demonstrating a positive correlation with the PCR data (Fig. 1h). Concurrent with the hepatic TDO2 expression was an increase in serum L-kynurenine-to-tryptophan ratios, an effect that was blocked by the TDO2 inhibitor 680C91, but not by *Ido1* deficiency (Fig. 1i).

To ascertain whether AhR expression correlated with functional activity, we measured induction of AhR-mediated gene transcription *ex vivo* in cells from WT mice, treated with 10 mg/kg LPS. Real-Time PCR was used to assess transcription of a gene (*Cyp1a1*) whose promoter contains xenobiotic response elements (Fig. 1j). *Cyp1a1* was induced in PECs and liver cells at 24 h, and this induction was dependent on TDO2 (and not on IDO1) and was restored in TDO2 inhibitor-treated mice by L-kynurenine, the first byproduct of tryptophan catabolism in the kynurenine pathway and an AhR signaling pathway inducer[16].

L-kynurenine is an endogenous AhR ligand

The nature of L-kynurenine as an AhR ligand[23] was preliminarily investigated in hepatocytes [which abundantly express the receptor] by binding competition experiments with [^{3}H]-2,3,7,8-tetrachlorodibenzo-*p*-dioxin (TCDD; Fig. 2a). Molecular modeling and docking studies, dynamics and free-energy calculations into a homology model of the PAS-B domain of AhR supported the ability of L-kynurenine to interact with the receptor, identifying Gln377 as a key residue involved in the effective binding of the ligand (i.e., *via* hydrogen bonds in the best energetic scored binding model). This residue was not previously reported as being part of the fingerprint residues necessary for the binding of TCDD to AhR[24] (Fig. 2b,c).

To substantiate the *in silico* data, a mutant AhR receptor was engineered carrying a Gln377Ala mutation (Q377A), and AhR-deficient cDCs were reconstituted with WT or mutated AhR. Transfection efficiency (≈ 50%) was similar for the two constructs, as revealed by staining with antibody recognizing both WT and mutant AhR on FACS

analysis. No differences in protein half-life (≈ 8 h) were found in cDCs reconstituted with either WT or Q377A AhR (Extended Data Fig. 3a; Extended Data Fig. 3b). When assayed for *Cyp1a1* transcriptional activity in cDCs reconstituted with mutated AhR, L-kynurenine exhibited complete loss of biologic activity, in terms of potency and likely affinity, compared to WT receptor-transfected counterparts (Fig. 2d). In contrast, on stimulation with TCDD, the 50% maximal effective concentration (EC_{50}) value of TCDD was approximately 20-fold lower when cells had been reconstituted with the mutated AhR (Fig, 2d), pointing to greater potency and affinity of the ligand for Q377A AhR. Competition by L-kynurenine for specific binding of [^{3}H]TCDD to cytosolic AhR from reconstituted *Ahr*$^{-/-}$ DCs allowed for an estimated L-kynurenine IC_{50} value of 36.2 μM and of 21.6 μM for K_i (Fig. 2e). Thus L-kynurenine and TCDD bind AhR with distinct affinities and exploit different types of interactions with AhR, either interaction involving a unique set of fingerprints residues necessary for effective binding.

AhR-deficient cDCs reconstituted with WT, but not Q377A, AhR transcriptionally expressed *Ido1* (Fig. 2f), *Il10* (Fig. 2g), and *Tgfb1* (Fig. 2h) in a dose-dependent manner in response to L-kynurenine, further underlining the crucial requirement for Gln377 in the AhR-dependent transcriptional activity in our setting. Cotrasfection of Q377A and WT AhR (but not a mock control) resulted in *Ido1*, *Il10* and *Tgfb1* transcription (Fig. 2f–h), suggesting that the mutant AhR did not interfere with WT AhR function. Altogether, these data supported the binding mode of L-kynurenine to AhR as predicted by docking studies, and they explained the AhR requirement for kynurenine induction of *Cyp1a1* transcription in PECs and liver cells (Fig. 2i).

When 200 mg/kg L-kynurenine (first-order elimination kinetics, $K_E = 0.023\ min^{-1}$; resulting in physiologically attainable concentrations in the low micromolar range) was administered to mice receiving 10 mg/kg LPS and the TDO2 inhibitor, all mice survived challenge, and this effect was negated by AhR deficiency (Fig. 2j). Overall, these data confirmed the crucial role of TDO2-dependent tryptophan catabolism in the activation of AhR necessary for downregulating inflammatory gene expression in primary endotoxemia. These data were also consistent with previous data in a different setting showing that L-kynurenine requires AhR in the absence of functional TDO2[25].

IDO1, AhR, and TGF-β are required for endotoxin tolerance

Next we examined the effect of high-dose LPS challenge in WT, IDO1-deficient or IDO2-deficient mice surviving a primary dose of 10 mg/kg LPS administered 1 wk earlier. Primed mice, as well as sham-tolerized controls of the different genotypes, received 40 mg/kg LPS i.p., to be monitored for mortality parameters (Fig. 3a). Only LPS-primed WT mice and *Ido2*$^{-/-}$ mice survived rechallenge beyond the 30-day observation period ($P < 0.0001$ *vs.* *Ido1*$^{-/-}$ and unprimed WT mice), as opposed to the rapid onset of a lethal shock in the other groups, whose median survival times were very similar (i.e., 24–48 h). Notably, under those conditions of primary LPS challenge (10 mg/kg), the LD_{50} of LPS-primed (i.e., tolerant) WT mice consistently exceeded 80 mg/kg, when estimated 1 wk after a first exposure to LPS. The LD_{50} values of primed *Ido1*$^{-/-}$ and unprimed WT mice were similar (27.1 and 33.9 mg/kg, respectively (Fig. 3b). Histopathology of lungs and liver showed that, at 48 h of

rechallenge with 40 mg/kg LPS, inflammation and neutrophil infiltration were similar in LPS-primed *Ido1*$^{-/-}$ mice and in IDO1-competent, unprimed controls (Fig. 3c,d).

After LPS rechallenge, increased transcriptional expression of *Ido1* and increased protein levels were demonstrable in splenic CD11c^{+} CD11b^{+} DCs (usually referred to as conventional DCs, or cDCs) and only marginally in peritoneal macrophages, and not at all in plasmacytoid DCs (pDCs) and peritoneal neutrophils (Extended Data Fig. 4a,b). LPS-primed WT and *Ido1*$^{-/-}$ cDCs promptly upregulated *Ahr* transcription upon LPS restimulation, yet this translated into enhanced AhR-dependent transcriptional activity only in IDO1-competent DCs, suggesting a necessary role for IDO1-dependent tryptophan catabolism in AhR-dependent gene transcription under those conditions of LPS rechallenge (Extended Data Fig. 4c). Likewise, the AhR requirement for endotoxin tolerance was demonstrated by the use of the specific antagonist, CH-223191 (Fig. 3e).

We also explored whether *Ahr*$^{-/-}$ mice could be tolerized by sublethal LPS amounts. The highest LPS dosage resisted by naive *Ahr*$^{-/-}$ mice (i.e., 0.5 mg/kg) would still confer some degree of endotoxin tolerance on WT but not AhR-deficient mice (Extended Data Fig. 5a). In contrast, TDO2 was not required for endotoxin tolerance, because inhibition of TDO2 at the time of LPS rechallenge with its selective inhibitor had no effects, and *Tdo2*$^{-/-}$ survivors of a primary LPS challenge would resist rechallenge to an extent comparable to primed WT controls (Extended Data Fig. 5b). Thus endotoxin tolerance, once established, did not require functional TDO2, but was dependent on the combined effects of IDO1 and AhR.

The early pattern of cytokine production by LPS-tolerant mice (at 2–24 h of rechallenge) was characterized by progressively decreasing levels of circulating TNF-α and IL-6, but sustained production of IL-10 and the appearance of circulating TGF-β, contingent on IDO1 (Fig. 3f). The cytokine secretion pattern of endotoxin-tolerant WT mice was in marked contrast with that of *Ido1*$^{-/-}$ mice, which resembled the cytokine secretion profile of unprimed WT controls (Fig. 3f). TGF-β was required for endotoxin tolerance because neutralization of TGF-β at the time of LPS rechallenge ablated protection (Fig. 3g). Increased serum tryptophan-to-kynurenine ratios were observed, on rechallenge, only in IDO1-competent mice (Fig. 3h).

In vivo, we investigated whether supplemental L-kynurenine – similar to what observed in the primary challenge of TDO2 KO mice with LPS – would be sufficient, alone, to reinstall tolerance in otherwise susceptible LPS-primed *Ido1*$^{-/-}$ mice. We treated mice with L-kynurenine at 6 h of LPS rechallenge (Fig. 3i). L-kynurenine failed to restore tolerance in the absence of IDO1, and there occurred a marked defect in TGF-β production in those mice, suggesting that IDO1 was required for circulating TGF-β production. Additional IDO1 functions, beside kynurenine production, might thus be required for establishing a fully protective endotoxin-tolerant state.

Endotoxin tolerance induces IDO1 phosphorylation which requires AhR

IDO1-dependent effects include nonenzymic functions, namely intracellular signaling events that, initiated by phosphorylation of specific domains in the enzyme, are involved in reprogramming gene expression and in the induction of a stably regulatory phenotype in

splenic pDCs[26]. Such polarized, tolerogenic pDCs produce less IL-6, but they start producing TGF-β in response to TLR signaling[27] or to TGF-β *in vitro*[28]. Because of the failure of supplemental L-kynurenine to confer significant endotoxin tolerance on LPS-primed *Ido1*$^{-/-}$ mice, we investigated whether IDO1-mediated signaling contributed to LPS tolerance, and in particular, whether IDO1 phosphorylation occurred in LPS-primed, IDO1-competent mice on rechallenge *in vivo* with LPS. We found that IDO1 phosphorylation could be detected under *ex vivo* conditions, in isolated spleen cells mostly expressing the CD11c marker, at 15 min of LPS rechallenge *in vivo* (Fig. 4a,b). Notably, IDO1 phosphorylation was not detected in the spleens of IDO1 KO mice. In accordance with the *ex vivo* data, AhR-dependent IDO1 phosphorylation could also be demonstrated in an *in vitro* model system using LPS-primed, IDO1-competent CD11c^{+} DCs on rechallenge with LPS (Fig. 4c).

To gain preliminary insight into the nature of the kinase responsible for the effect, we searched cDC gene expression profiles in public data sets, focusing on Src kinases known to mediate tyrosine-phosphorylation of intracellular target proteins. Profile analysis indicated that, among several possibilities including *Sykb*, *Blk*, *Frk*, *Zap70*, *Fgr*, *Fyn*, *Hck*, *Lck*, *Lyn*, *Src*, *Yes1* and *Csk*, the most widely represented kinase in mouse LPS-treated cDCs was the product of *Src* (Extended Data Fig. 6a,b). Src kinase activity is triggered by AhR activation[29,30], resulting in autophosphorylation and phosphorylation of target proteins[31]. Early, Src-dependent phosphorylation of IDO1 in primed cDCs occurred in response to LPS, and inhibition of Src kinase using a selective inhibitor, PP2 – but not its inactive analog, PP3 – negated IDO1 phosphorylation in LPS-primed cDCs re-exposed to LPS (Fig. 4c). Also, Src activity required AhR (Fig. 4d), which was necessary for TGF-β production (Fig. 4e). Overall, these data indicated that, in endotoxin tolerance, AhR-associated Src activity is responsible for IDO1 phosphorylation and TGF-β production by IDO1-competent cDCs.

Endotoxin tolerance protects against *Salmonella* infection

TLR4 and TLR2 activate innate immune cells in response to gram-negative and gram-positive bacteria, respectively. We first analyzed the impact of endotoxin tolerance on acute infection with LPS-expressing *Salmonella enterica* Typhimurium (*S.* Typhimurium, which exploits intestinal inflammation for pathogenicity[32]). Mice were treated once with LPS (10 mg/kg; day -7) and then rechallenged with LPS (40 mg/kg) two days before intragastric infection with 1×10^7 *S.* Typhimurium cells (day 0). At 2 days post infection, the cecum was heavily colonized in all groups, with mice treated once with LPS showing a higher colonization (Fig. 5a). Stained cecal tissue sections showed that the infected tissues were characterized by extensive submucosal edema, thickened mucosa, and inflammatory cell recruitment, which effects were ameliorated by double LPS exposure (Fig. 5b). In cecum cell supernatants, IL-6, and TNF-α were significantly affected by LPS rechallenge. TGF-β was increased by the same treatment regimen, and no differences were observed for IL-10 (Fig. 5c).

By day 14 post infection in LPS-tolerant mice, bacterial counts in the cecum were reduced by LPS administered twice (Fig. 5d). On gross histopathology, the cecum and distal colon of vehicle-treated mice appeared thickened with an increase in weight, as compared to mice on

effective treatment (Fig. 5d,e). Reduced inflammatory pathology was confirmed by lower levels of IL-1β and TNF-α in cecum cell supernatants (Extended Data Fig. 7a). Moreover, higher levels of IL-10 and TGF-β were found in those mice (Extended Fig. 7a), in which *Foxp3* expression in mesenteric lymph nodes was enhanced, as opposed to *Rorc* expression (Extended Fig. 7b).

Because AhR and IDO1 were required for fully protective tolerance in this model system, we also investigated whether AhR and IDO1 were involved in the spontaneous resistance to *Salmonella* infection. We found that naïve AhR- or IDO1-deficient mice showed increased susceptibility than WT controls to *S*. Typhimurium challenge, in terms of survival ($Ahr^{-/-}$) as well as histopathology, with the infected tissues being characterized by extensive submucosal edema, thickened mucosa, and inflammatory cell recruitment, and T_H17/Treg cell imbalance (both $Ahr^{-/-}$ and $Ido1^{-/-}$ mice; Extended Data Fig. 8a–c). Thus AhR and IDO1 are also involved in the resistance of naïve mice to challenge with an LPS-expressing pathogen.

Endotoxin tolerance protects against group B *Streptococcus* -induced septic arthritis

Next, we evaluated the impact of endotoxin tolerance on group B *Streptococcus* (GBS)-induced multifocal septic arthritis, a condition in which functional TLR2 signaling is necessary for attenuating the severity of group B streptococcal disease[33]. Mice preconditioned as in the *Salmonella* model were infected i.v. with 1×10^7 type IV group B streptococci, and disease severity was monitored by assessing both survival rates and clinical scores of arthritis. Mice receiving LPS twice displayed improved survival (Fig. 6a). In those mice, there occurred a significantly ($P < 0.05$) lower frequency as well as a lower severity of articular lesions with respect to mice receiving LPS only once, or to vehicle-treated mice (Fig. 6b). In particular, a maximum of 25% incidence was observed in mice on repeated LPS exposure on day 10 after infection (Fig. 6b), never exceeding an arthritis index of 0.5 ± 0.2. The protective effects of double LPS exposure was reflected in a decreased bacterial burden in the kidneys and joints on days 5 and 10 post infection (Fig. 6c). Histopathology findings confirmed the clinical data. The totality of joints from vehicle-treated mice, and 88% of those receiving LPS once, showed histological features of arthritis, and most of them were classified as severely or moderately affected. In contrast, all joints from LPS-tolerant mice showed no signs of arthritis (Fig. 6d). The levels of proinflammatory cytokines, particularly IL-6, IL-1β and IL-17A in inflamed joints and sera were dramatically decreased in mice on effective treatment. Moreover, production of IL-10 and TGF-β was boosted by repeated LPS treatment, in inflamed joint supernatants (Fig. 6e). Endotoxin tolerance increased *Foxp3* and decreased *Rorc* expressions in joint-draining lymph nodes (Extended Data Fig. 9). Naïve AhR- or IDO1-deficient mice showed increased susceptibility than WT mice to GBS challenge and associated immunopathology (Extended Data Fig. 10 a–c).

Discussion

We found that overreacting responses to primary LPS challenge are controlled by AhR, TDO2, and IL-10, whereas endotoxin tolerance requires the combined effects of AhR,

IDO1, and TGF-β. In particular, the IDO1-dependent, systemic regulatory response resulting in endotoxin tolerance appears to be part of a series of sequential events, to which AhR contributes distinct effects, mostly occurring in cDCs. These are converted to a stably regulatory phenotype by the combined actions of AhR, activated by tryptophan metabolites, and of phosphorylated IDO1, in a TGF-β–dominated network. We have, indeed, obtained evidence for *a)* requirement for IDO1 and AhR activation for endotoxin tolerance to become established; *b)* phosphorylation of IDO1 by Src, belonging in the AhR complex; and *c)* sustained production of TGF-β, requiring phosphorylated IDO1 for establishing durable tolerance[34]. Not secondarily, our data also show that *d)* functionally distinct AhR ligands, such as TCDD and L-kynurenine, bind AhR through ligand-specific interactions, each requiring a unique set of fingerprint residues and each initiating a distinct pathway of downstream signaling and transcriptional events.

Several considerations may apply, in a broader context, to the above findings. Firstly, our data suggest that, although the class of an immune response is tailored to fit the invading pathogen, its regulation is primarily tailored to fit the tissue in which the response occurs[35,36]. Secondly, endotoxin tolerance can be seen as a form of protective[37] or infectious[38] tolerance, whereby the host organism protects itself from infectious diseases by reducing the negative impact of infections on host fitness, an ability epitomized by Medzhitov *et al*. as “disease tolerance”[39]. While disease resistance aims at reducing or eliminating infection, disease tolerance is confirmed here to imply an ability to reduce the impact of infection on host fitness. In the third place, the IDO1 mechanism appears to have been selected through phylogenesis primarily to prevent overreacting responses to TLR-recognized pathogen-associated molecular patterns[40], and only later did it become involved in the response to T cell receptor-recognized antigen[15,26].

AhR, in turn, which has a role in regulatory T-cell generation[17], is presumed to have evolved from invertebrates, where it served a ligand-independent role in normal development processes. Evolution of the receptor in vertebrates resulted in the ability to bind structurally different ligands, including xenobiotics and microbiota-derived catabolites[45]. Considering the inability of invertebrate AhR homologs to bind dioxins, the adaptive role of the AhR to act as a regulator of xenobiotic-metabolizing enzymes may have been a vertebrate innovation, to later acquire an additional immune regulatory role by coevolutive pressure in mammals by IDO1 and regulatory T cells[41-44]. Although *Ahr*$^{-/-}$ mice have already been described as manifesting increased susceptibility to endotoxemia[10], our data on the respective inabilities of TDO2 KO and IDO1 KO mice to mount protective responses to LPS challenge and rechallenge may be the first to document uncompensated immune deficits in those mice.

AhR would, indeed, engage in the long-term regulation of systemic, TLR-triggered inflammation through IDO1, resulting in the onset of a fully protective endotoxin-tolerant state, as exemplified by the *Salmonella* infection model. It is, however, possible that the immunoregulatory effects of tryptophan catabolism represent a generalized phenomenon in infection and infection-related pathology[46]. Our findings in the *Streptococcus* -induced septic arthritis model demonstrate that endotoxin tolerance does not prevent the early events in protective TLR2 signaling, and it may, in fact, accelerate the later onset of host’s control

over immunologically mediated local and systemic disease. This would suggest that endotoxin tolerance helps to control specific, inflammasome-mediated effects of bacterial infection[47].

Interfering with the trade-offs that the defense systems in both pathogens and their hosts impose on host fitness could ultimately help to selectively enhance pathways responsible for strong and rapid inflammatory responses that lead to effective pathogen clearance, yet do not involve immunopathology[48]. Our current data may pave the way to new therapeutic options in infectious diseases *via* control of host-pathogen interactions. Druggable candidate targets in those interactions may include sensors of pathogen presence, such as TLRs, alterations of host metabolism – including tryptophan catabolism – and environment responsive receptors (e.g., AhR). In addition, genes controlling regulatory pathways, tissue repair and resolution are also tolerance candidates.

METHODS

Mice

Eight- to ten-week-old male C57BL/6 mice were obtained from Charles River Breeding Laboratories. IDO1 deficient mice (*Ido1*$^{-/-}$) were purchased from The Jackson Laboratory. B6.129-Ahrtm1Bra/J mice deficient for *Ahr* (*Ahr*$^{-/-}$) were kindly supplied by B. Stockinger (MRC National Institute for Medical Research, London, UK); IDO2 deficient mice (*Ido2*$^{-/-}$) mice were bred at Lankenau Institute for Medical Research, Wynnewood, PA, USA, and TDO2 deficient (*Tdo2*$^{-/-}$) mice were bred in H. Funakoshi's laboratory (Center for Advanced Research and Education, Asahikawa Medical University, Japan). All other mice were bred at the animal facility of the University of Perugia.

LPS-induced endotoxemia tolerance and treatments

In the induction of primary endotoxemia, mice of the different genotypes were randomly grouped (10 per group) and injected i.p. with different doses of LPS (in a final volume of 200 μl; Sigma #055:B5). LD_{50} values for each genotype were calculated by curve fitting (r^2 > 0.96–0.99) and data are from one experiment representative of two (Fig. 1c) or three (Fig. 3b). In the tolerance experiments, mice were injected i.p. with a first dose of LPS (10 mg/kg) and, after 6 days, rechallenged with 40 mg/kg LPS. Groups of mice received neutralizing antibodies to IL-10 (200 μg/mouse) or TGF-β (11D1; 100 μg/mouse), or recombinant IL-10 (250 ng /mouse), isotype-matched antibodies serving as control treatments. 1-MT (5 mg per mouse; D,L racemic mixture; Sigma) was administered i.p., and 680C91 (5 mg/kg; R&D Systems) was administered by oral gavage 3 h before LPS administration and then for three consecutive days. CH-223191 (10 mg/kg) was administered by oral gavage starting one day after the first LPS administration and then daily up to LPS rechallenge. Vehicle-treated groups were used as controls. Mice was checked for mortality and autopsied every 12 h for 7 days.

Reagents

Rabbit monoclonal anti-mouse IDO1 antibody (cv152) was as described[18] and so was the rabbit polyclonal anti–phospho-IDO1 (anti-pIDO1)[28]. Rabbit anti-mouse IDO2

(unrecognizing IDO1 epitopes) was raised in our laboratory to an IDO2-specific synthetic peptide (GLKALVQ, GMEAIRQHSRDT, ISAATRARSRGLTNPSPHA) and purified by affinity chromatography. The following antibodies were also used, anti-mouse AhR (R&D Systems and Abcam), anti-mouse TDO2 (a gift from C. L. Miller, Johns Hopkins University, Baltimore, MD), anti-mouse Src and Phospho-Src Family (Tyr416; Cell Signaling), and anti-mouse β-tubulin (Sigma-Aldrich). The Src inhibitor PP2 and its negative control, PP3, were from Tocris Bioscience.

Isolation of macrophages, neutrophils and dendritic cells, and treatments

Mouse peritoneal macrophages were collected from euthanized animals, and purified according to standard procedures. Cells were >99% $CD11b^+$, >99% $F480^+$, <0.1% $CD3^+$, <0.1% $B220^+$. Neutrophils were isolated from the peritoneal cavity *via* biotin-labeled anti-Ly6G, by magnetic separation using anti-biotin magnetic beads according to manufacturer's instructions (Miltenyi Biotec). Neutrophils were defined as being $CD11b^{high}$ $Ly6G^{high}$. Splenic DCs were purified using CD11c MicroBeads (Miltenyi Biotec) in the presence of EDTA to disrupt DC-T cell complexes. Cells were >99% $CD11c^+$, >99% MHC $I\text{-}A^+$, >98% $B7\text{-}2^+$, <0.1% $CD3^+$, and appeared to consist of 90–95% $CD8^-$, 5–10% $CD8^+$, and 1–5% $B220^+$ cells. DC populations were further fractionated according to CD8 or mPDCA-1 expression to obtain purified $CD8^-$ DCs (cDCs) or $mPDCA\text{-}1^+$ pDCs, by means of selective MicroBeads (Miltenyi Biotec). In accordance with our previous data[15,28], the $CD8^-$ fraction was 45% $CD4^+$ and typically contained <0.5% contaminating $CD8^+$ cells, whereas >95% of the $mPDCA\text{-}1^+$ cells were also positive on 120G86 antibody staining. For *in vitro* studies, cDCs (1×10^6 cells per well in 24-well plates) were cultured for 24 h with medium or with LPS (0.5 μg/ml; on first LPS exposure); when indicated, they were washed and restimulated for an additional 6–24 h with LPS (1 μg/ml). For TGF-β neutralization, cDCs were incubated with 1D11 mAb (40 μg/ml). In specific *in vitro* experiments, PP2 (5 μM) or PP3 (5 μM) were added 1 h before LPS treatment.

Real-Time RT-PCR

Real-Time RT-PCR (for mouse *Ido1*, *Ido2*, *Tdo2*, *AhR*, *Il10*, *Tgfb1* and *Gapdh)* analyses were carried out as described[28], using primers listed in Extended Data Table 1. Liver homogenate was used as a positive control for expression of *Tdo2*, *Ido2*, *Ahr*, and *Cyp1A1*. RT-PCR data were calculated as the ratio of gene to *Gapdh* expression by the relative quantification method (ΔΔCT; means ± s.d. of triplicate determination), and data are presented as normalized transcript expression in the samples relative to normalized transcript expression in control cultures (in which fold change = 1; dotted line).

ELISA

Mouse cytokines (IL-6, IL-1β, IL-10, TNF-α, TGF-β1, and IL-17A) were measured in serum or culture supernatants by ELISA using specific kits (R&D Systems and Abnova Corporation) or previously described reagents and procedures[28,49]. The detection limits (pg/ml) of the assays were 2 for IL-6, IL-10, IL-1β and IL-17A, and 15 for TGF-β1.

AhR binding studies

[^{3}H]-2,3,7,8-tetrachlorodibenzo-*p*-dioxin ([^{3}H]TCDD) (37 Ci/mmole) and 2,3,7,8-tetrachlorodibenzofuran (TCDF) were obtained from Accustandards. Hepatic cytosol was prepared from male C57BL/6 mouse livers in HEDG buffer (25 mM Hepes, pH 7.5, 1 mM EDTA, 1 mM dithiothreitol, and 10% (v/v) glycerol), as previously described for guinea pig preparations[50] and was stored at −80 °C until use. After protein normalization, measurement of AhR ligand binding was carried out using the sucrose gradient centrifugation assay. Cytosol (5 mg protein/ml) was incubated with 5 nM [^{3}H]TCDD in the presence of DMSO (10 μl/ml), 1 μM TCDF, or 100 μM kynurenine for 1 h at 4 °C. After treatment with dextran-coated charcoal to remove unbound and loosely bound radioligand, samples were subjected to centrifugation in linear 10–30% sucrose (v/v) gradients at 65,000 rpm for 2 h at 4 °C. Following centrifugation, gradients were fractionated and the radioactivity present in each fraction was determined by liquid scintillation. Specific binding of [^{3}H]TCDD to AhR was determined by subtraction of the amount of [^{3}H]TCDD bound in the presence of control TCDF or of kynurenine from the amount of [^{3}H]TCDD bound in the absence of any competitor. Mouse hepatic cytosol was incubated with labeled TCDD. In Fig. 2a, the total amount of [^{3}H]TCDD-specific binding activity (mean ± s.d.) in three experiments was 99.4 ± 3.2 fmoles/mg protein, of which 99.6 ± 1.5 percent was displaced by 100 μM kynurenine. In Fig. 2e, a ligand binding competition assay was performed essentially as previously described[50] and adapted for mouse DCs. Cytosolic cell extracts from mouse *Ahr*$^{-/-}$ cDCs, reconstituted with WT Ahr, were prepared by suspending cell pellets in HEDG buffer [25 mM Hepes, 1 mM EDTA, 1 mM dithiothreitol, and 10% (v/v) glycerol, pH 7.5] containing a commercial protease inhibitor. Aliquots of the supernatant (100 μg) were incubated at room temperature for 2 h with the indicated concentrations of kynurenine in the presence of 0.3 nM [3H]TCDD in HEDG buffer. After incubation on ice with hydroxyapatite for 30 min, HEDG buffer with 0.5% Tween 80 was added. The samples were centrifuged, washed twice, resuspended in 0.2 ml scintillation fluid, and subjected to scintillation counting. Nonspecific binding was determined using a 150-fold molar excess of TCDF and subtracted from the total binding to obtain the specific binding. The specific binding is reported relative to [3H]TCDD alone. The equilibrium inhibitor constant K_i was calculated based on the formula, $K_i = IC_{50}/(1 + [L]/K_{d_L}$ where L designates the radioligand.

Molecular Modeling

A multiple alignment between the sequences of PAS-B mAhR (residues 278–384) and PAS-B HIF-2α was generated according to the sequence alignment suggested by Pandini *et al*[24]. The homology model of PAS-B mAhR was constructed using the crystal structures of the heterodimer complex of PAS-B HIF-2α (pdb code: 3f1p, 3f1o, 3f1n) and Prime v.2.1. L-kynurenine was built in the zwitterionic form using the ligand preparation tool from Maestro. Docking experiments were carried out using Glide v5.9 and the QM-polarized ligand docking procedure. The best energetic scored solution was selected for the analysis of the binding mode of L-kynurenine to AhR.

Luciferase assays

AhR-deficient cDCs (10×10^6), reconstituted either with WT or Q377A AhR, were electroporated (230 V, 75 Ohm and 1,500 microfarads) in Optimem/Glutamax (Invitrogen) with 30 μg of the firefly luciferase reporter pGudLuc1.1 plasmid, which contains a 480 bp fragment of the upstream enhancer region of the mouse *Cyp1a1* gene – including four xenobiotic response elements – upstream of the firefly luciferase coding sequence. Another reporter plasmid, pRL-TK (1 μg; Promega) encoding *Renilla* luciferase, was electroporated as an internal control of the transfection process. Cells were seeded in 24-well plates at a density of 1.2×10^6 cells/ml. After 2 h at 37 °C, cells were stimulated for 8–10 h with increasing concentrations of TCDD, as the reference AhR ligand, or L-kynurenine before lysis. Luciferase assays were performed using the dual luciferase reporter assay kit (Promega). In Fig. 2d, cells were treated with TCDD or kynurenine, the ratio of firefly to *Renilla* luciferase activity was measured, and results are presented as fold induction. In Fig. 2f–h, AhR-deficient cDCs were reconstituted with AhR WT or AhR bearing the Q377A mutation, (or the empty vector as a control; mock) or co-transfected with equal amounts of Q377A mutant AhR and WT AhR, or equal amounts of Q377A and the control vector. After reconstitution, cells were treated with kynurenine at different concentrations and assayed for their ability to induce *Ido1*, *Il10* and *Tgfb1* transcripts at 24 h. Data are presented as normalized transcript expression in the samples relative to normalized transcript expression in mock-transfected, AhR-deficient cDCs treated with the respective kynurenine concentration, in which fold change = 1.

Expression levels of tyrosine kinases in mouse myeloid dendritic cells

We retrieved seven datasets of mouse myeloid dendritic cells from Gene Expression Omnibus (http://www.ncbi.nlm.nih.gov/geo), containing information about treatment with LPS and gene expression data obtained with Affymetrix Mouse Genome 430 2.0 arrays (Extended Data Table 2). After manual re-annotation, all samples were merged into a meta-dataset and analyzed to derive gene expression profiles for a set of 13 tyrosine kinases. Since raw data (e.g., CEL files) were available for all samples, expression values of the meta-dataset were generated from fluorescence signals using the robust multi-array average procedure[28]. Specifically, intensity levels were background-adjusted, normalized using quantile normalization, and $\log_2$ expression values calculated using median polish summarization and Entrez custom chip definition files for mouse arrays. The expression change of any tyrosine kinase was quantified as the difference between its average $\log_2$ gene expression signal in untreated samples and its $\log_2$ expression level in any specimen stimulated with LPS ($\log_2$ fold-change). Extended Data Fig. 6a,b depicts the fold changes of tyrosine kinases in LPS samples (as compared to untreated myeloid dendritic cells) as a mean value with standard error of the mean.

Phosphorylation of IDO1

Phosphorylation was examined in total splenocytes isolated from WT mice, either unprimed or primed *in vivo* with LPS (10 mg/kg), with or without rechallenge with 40 mg/kg LPS on day +7. Kinetic assessment was done by sequential immunoblotting with anti-pIDO1 (specifically recognizing the phosphorylated ITIM2 motif in IDO1), an anti-IDO1 reagent,

and anti–β-tubulin for normalization. Ratios of pIDO1 to IDO1 were determined by analyzing bands (as normalized to β-tubulin) with image J software. Splenic immunofluorescent staining was done with PE-CD11c and anti-IDO1 or anti–pIDO1, followed by FITC-conjugated antibody. Cell nuclei stained blue with DAPI. Representative images were taken using a high-resolution Microscopy Olympus DP71 (×40 magnification). Phosphorylation of IDO1's ITIM2 in WT and AhR-deficient cDCs was done using cells either unprimed or primed *in vitro* with of LPS (1 μg/ml) and then restimulated with an equal LPS concentration. Kinetic assessment was done by sequential immunoblotting with anti-pIDO1 (specifically recognizing the phosphorylated ITIM2 motif in IDO1), an anti-IDO1 reagent, and anti–β-tubulin for normalization. Samples included cDCs pretreated for 1 h with an Src inhibitor (PP2), or its inactive control (PP3), before the second LPS exposure, and IDO1 phosphorylation was assessed at 30 min.

Immunofluorescence

For immunohistochemistry, the spleen was removed and fixed in 10% phosphate-buffered formalin, embedded in paraffin and sectioned at 5 μm. Sections were then rehydrated and after antigen retrieval in Citrate Buffer (10mM, pH6), sections were blocked with 5% BSA in PBS and stained with PE-CD11c (eBioscience, San Diego, CA) and anti-IDO1 (5 μg/ml) or anti–phospho-IDO1 (5 μg/ml) followed by secondary FITC-conjugated mouse anti–rabbit antibody (Sigma Aldrich). All mAbs were incubated overnight at 4 °C. Cells were counterstained with DAPI (4'-6-diamino-2-phenylindole, Molecular Probes, Invitrogen) to detect nuclei. Immunofluorescence microscopy was performed on an Olympus microscope (BX51) and analySIS image processing software.

Histology and L-kynurenine determination

Morphological investigation the lungs, livers and ceca of mice treated with different doses of LPS or L-kynurenine were as described[33], and so were measurements of IDO1 functional activity in terms of L-kynurenine production[18]. In Fig. 1d,e immune cells and tissue damage (arrows) in livers were revealed by H&E staining at 48 h of challenge, using representative specimens from one of three experiments.

Salmonella infection model

S. enterica Typhimurium strain ΔaroA was grown overnight in Luria-Bertani broth containing 100 μg/ml streptomycin without shaking at 37 °C, and diluted in PBS after estimation of bacterial concentration using a spectrophotometer. Mice received 20 mg streptomycin by oral gavage followed by infection with 1×10^7 *S.* Typhimurium bacteria, then closely monitored for signs of infection. Mice were sacrificed at 2 and 14 days post infection. Cecum and distal colon were collected, photographed, measured and weighed. To determine the bacterial colonization *in vivo*, the cecum and spleen from infected mice were homogenized in PBS and serial dilutions were plated onto MacConkey agar plates. After overnight incubation at 37 °C, plates were counted and bacterial numbers calculated for each individual organ sample.

Streptococcus infection arthritis model

All procedures have been described elsewhere in full detail[33]. Briefly, WT mice, either unprimed or primed once or twice with LPS, were infected with 1×10^7 CFU of group B streptococci. Survival was recorded at 24-h intervals for 20 days, and the arthritis index (expressing clinical severity of arthritis) was evaluated daily over the same timeframe, along with CFU (mean values ± s.d.) in joints and kidneys. At the indicated times, three mice per group were sacrificed and organ homogenates were spread on blood agar plates for GBS load assessment.

Statistical analysis

The log-rank test was used for paired data analyses of Kaplan-Meier survival curves. Linear regression analysis of individual disease curves was carried out using the mean clinical score as the dependent variable and time (days) as the independent variable. All *in vitro* determinations are means ± s.d. from three independent experiments, and were evaluated by Shapiro test and two-tailed Student's *t*-test, as appropriate. All *n* values were computed by power analysis to yield a power of at least 80% with an α-level of 0.05. GraphPad Prism version 6.0 (San Diego, CA) was used for all analyses, including calculations of median lethal doses of LPS *in vivo* and half-maximal effective concentrations *in vitro*, and graph preparation.

Supplementary Material

Refer to Web version on PubMed Central for supplementary material.

Acknowledgments

This work was supported by funding from the Italian Association for Cancer Research (AIRC, to P.P.), *Fondazione Italiana Sclerosi Multipla* Project No. 2010/R/17 (to F.F.), *Associazione Umbra Contro il Cancro* (to G.S. & M.A.D.F.), Bayer Hemophilia Award grant 2011 (to D.M. & F.F.), Bayer Early Career Investigator Award (to D.M.), Grant #R01ES007685 from the U.S. National Institutes of Environmental Health Sciences (to M.D.), the Specific Targeted Research Project FUNMETA (to L.R.), and the Italian Ministry of Health in association with *Regione dell'Umbria* (GR-2008-1138004 to C.O.) We thank G. Andrielli for digital art and image editing and Dr. Giovanni Ricci (University of Perugia) for histopathology.

References

1. Fan H, Cook JA. Molecular mechanisms of endotoxin tolerance. J. Endotoxin. Res. 2004; 10:71–84. [PubMed: 15119998]
2. Pena OM, Pistolic J, Raj D, Fjell CD, Hancock RE. Endotoxin tolerance represents a distinctive state of alternative polarization (M2) in human mononuclear cells. J. Immunol. 2011; 186:7243–7254. [PubMed: 21576504]
3. Krausgruber T, et al. IRF5 promotes inflammatory macrophage polarization and T_H1-T_H17 responses. Nat. Immunol. 2011; 12:231–238. [PubMed: 21240265]
4. Abdi K, Singh NJ, Matzinger P. Lipopolysaccharide-activated dendritic cells: "exhausted" or alert and waiting? J. Immunol. 2012; 188:5981–5989. [PubMed: 22561154]
5. Biswas SK, Lopez-Collazo E. Endotoxin tolerance: new mechanisms, molecules and clinical significance. Trends Immunol. 2009; 30:475–487. [PubMed: 19781994]
6. Park SH, Park-Min KH, Chen J, Hu X, Ivashkiv LB. Tumor necrosis factor induces GSK3 kinase-mediated cross-tolerance to endotoxin in macrophages. Nat. Immunol. 2011; 12:607–615. [PubMed: 21602809]

7. Doreswamy V, Peden DB. Modulation of asthma by endotoxin. Clin. Exp. Allergy. 2011; 41:9–19. [PubMed: 20977505]
8. Stejskalova L, Dvorak Z, Pavek P. Endogenous and exogenous ligands of aryl hydrocarbon receptor: current state of art. Curr. Drug Metab. 2011; 12:198–212. [PubMed: 21395538]
9. Quintana FJ. The aryl hydrocarbon receptor: a molecular pathway for the environmental control of the immune response. Immunology. 2013; 138:183–189. [PubMed: 23190340]
10. Kimura A, et al. Aryl hydrocarbon receptor in combination with Stat1 regulates LPS-induced inflammatory responses. J. Exp. Med. 2009; 206:2027–2035. [PubMed: 19703987]
11. Nguyen LP, Bradfield CA. The search for endogenous activators of the aryl hydrocarbon receptor. Chem. Res. Toxicol. 2008; 21:102–116. [PubMed: 18076143]
12. Murray MF. The human indoleamine 2,3-dioxygenase gene and related human genes. Curr. Drug Metab. 2007; 8:197–200. [PubMed: 17430106]
13. Orabona C, et al. Toward the identification of a tolerogenic signature in IDO-competent dendritic cells. Blood. 2006; 107:2846–2854. [PubMed: 16339401]
14. Stone TW, Stoy N, Darlington LG. An expanding range of targets for kynurenine metabolites of tryptophan. Trends Pharmacol. Sci. 2013; 34:136–143. [PubMed: 23123095]
15. Fallarino F, et al. The combined effects of tryptophan starvation and tryptophan catabolites down-regulate T cell receptor ζ-chain and induce a regulatory phenotype in naive T cells. J. Immunol. 2006; 176:6752–6761. [PubMed: 16709834]
16. Nguyen NT, et al. Aryl hydrocarbon receptor negatively regulates dendritic cell immunogenicity via a kynurenine-dependent mechanism. Proc. Natl. Acad. Sci. U S A. 2010; 107:19961–19966. [PubMed: 21041655]
17. Mezrich JD, et al. An interaction between kynurenine and the aryl hydrocarbon receptor can generate regulatory T cells. J. Immunol. 2010; 185:3190–3198. [PubMed: 20720200]
18. Romani L, et al. Defective tryptophan catabolism underlies inflammation in mouse chronic granulomatous disease. Nature. 2008; 451:211–215. [PubMed: 18185592]
19. Changsirivathanathamrong D, et al. Tryptophan metabolism to kynurenine is a potential novel contributor to hypotension in human sepsis. Crit. Care Med. 2011
20. Jung ID, et al. Blockade of indoleamine 2,3-dioxygenase protects mice against lipopolysaccharide-induced endotoxin shock. J. Immunol. 2009; 182:3146–3154. [PubMed: 19234212]
21. Sekine H, et al. Hypersensitivity of aryl hydrocarbon receptor-deficient mice to lipopolysaccharide-induced septic shock. Mol. Cell. Biol. 2009; 29:6391–6400. [PubMed: 19822660]
22. Trifari S, Kaplan CD, Tran EH, Crellin NK, Spits H. Identification of a human helper T cell population that has abundant production of interleukin 22 and is distinct from T_H-17, T_H1 and T_H2 cells. Nat. Immunol. 2009; 10:864–871. [PubMed: 19578368]
23. Howard GJ, Schlezinger JJ, Hahn ME, Webster TF. Generalized concentration addition predicts joint effects of aryl hydrocarbon receptor agonists with partial agonists and competitive antagonists. Environ. Health Perspect. 2010; 118:666–672. [PubMed: 20435555]
24. Pandini A, et al. Detection of the TCDD binding-fingerprint within the Ah receptor ligand binding domain by structurally driven mutagenesis and functional analysis. Biochemistry. 2009; 48:5972–5983. [PubMed: 19456125]
25. Opitz CA, et al. An endogenous tumour-promoting ligand of the human aryl hydrocarbon receptor. Nature. 2011; 478:197–203. [PubMed: 21976023]
26. Fallarino F, Grohmann U, Puccetti P. Indoleamine 2,3-dioxygenase: from catalyst to signaling function. Eur. J. Immunol. 2012; 42:1932–1937. [PubMed: 22865044]
27. De Luca A, et al. Functional yet balanced reactivity to Candida albicans requires TRIF, MyD88, and IDO-dependent inhibition of Rorc. J. Immunol. 2007; 179:5999–6008. [PubMed: 17947673]
28. Pallotta MT, et al. Indoleamine 2,3-dioxygenase is a signaling protein in long-term tolerance by dendritic cells. Nat. Immunol. 2011; 12:870–878. [PubMed: 21804557]
29. Dong B, et al. FRET analysis of protein tyrosine kinase c-Src activation mediated via aryl hydrocarbon receptor. Biochim. Biophys. Acta. 2011; 1810:427–431. [PubMed: 21145940]

30. Randi AS, et al. Hexachlorobenzene triggers AhR translocation to the nucleus, c-Src activation and EGFR transactivation in rat liver. Toxicol. Lett. 2008; 177:116–122. [PubMed: 18295415]
31. Backlund M, Ingelman Sundberg, M. Regulation of aryl hydrocarbon receptor signal transduction by protein tyrosine kinases. Cell. Signal. 2005; 17:39–48. [PubMed: 15451023]
32. Thiennimitr P, et al. Intestinal inflammation allows Salmonella to use ethanolamine to compete with the microbiota. Proc. Natl. Acad. Sci. U S A. 2011; 108:17480–17485. [PubMed: 21969563]
33. Puliti M, Uematsu S, Akira S, Bistoni F, Tissi L. Toll-like receptor 2 deficiency is associated with enhanced severity of group B streptococcal disease. Infect. Immun. 2009; 77:1524–1531. [PubMed: 19179417]
34. Chen W. IDO: more than an enzyme. Nat. Immunol. 2011; 12:809–811. [PubMed: 21852775]
35. Matzinger P, Kamala T. Tissue-based class control: the other side of tolerance. Nat. Rev. Immunol. 2011; 11:221–230. [PubMed: 21350581]
36. Sander LE, et al. Hepatic acute-phase proteins control innate immune responses during infection by promoting myeloid-derived suppressor cell function. J. Exp. Med. 2010; 207:1453–1464. [PubMed: 20530204]
37. Romani L, Puccetti P. Protective tolerance to fungi: the role of IL-10 and tryptophan catabolism. Trends Microbiol. 2006; 14:183–189. [PubMed: 16517165]
38. Belladonna ML, Orabona C, Grohmann U, Puccetti P. TGF-β and kynurenines as the key to infectious tolerance. Trends Mol. Med. 2009; 15:41–49. [PubMed: 19162548]
39. Medzhitov R, Schneider DS, Soares MP. Disease tolerance as a defense strategy. Science. 2012; 335:936–941. [PubMed: 22363001]
40. Volpi C, et al. High doses of CpG oligodeoxynucleotides stimulate a tolerogenic TLR9-TRIF pathway. Nat. Commun. 2013; 4:1852. [PubMed: 23673637]
41. Grohmann U, et al. CTLA-4-Ig regulates tryptophan catabolism in vivo. Nat. Immunol. 2002; 3:1097–1101. [PubMed: 12368911]
42. Fallarino F, et al. Modulation of tryptophan catabolism by regulatory T cells. Nat. Immunol. 2003; 4:1206–1212. [PubMed: 14578884]
43. Munn DH, et al. Prevention of allogeneic fetal rejection by tryptophan catabolism. Science. 1998; 281:1191–1193. [PubMed: 9712583]
44. Samstein RM, Josefowicz SZ, Arvey A, Treuting PM, Rudensky AY. Extrathymic generation of regulatory T cells in placental mammals mitigates maternal-fetal conflict. Cell. 2012; 150:29–38. [PubMed: 22770213]
45. Zelante T, et al. Tryptophan catabolites from microbiota engage aryl hydrocarbon receptor and balance mucosal reactivity via interleukin-22. Immunity. 2013; 39:372–385. [PubMed: 23973224]
46. Zelante T, Fallarino F, Bistoni F, Puccetti P, Romani L. Indoleamine 2,3-dioxygenase in infection: the paradox of an evasive strategy that benefits the host. Microbes Infect. 2009; 11:133–141. [PubMed: 19007906]
47. Martinon F, Mayor A, Tschopp J. The inflammasomes: guardians of the body. Ann. Rev. Immunol. 2009; 27:229–265. [PubMed: 19302040]
48. Chambers MC, Schneider DS. Balancing resistance and infection tolerance through metabolic means. Proc. Natl. Acad. Sci. U S A. 2012; 109:13886–13887. [PubMed: 22891309]
49. Orabona C, et al. SOCS3 drives proteasomal degradation of indoleamine 2,3-dioxygenase (IDO) and antagonizes IDO-dependent tolerogenesis. Proc. Natl. Acad. Sci. USA. 2008; 105:20828–20833. [PubMed: 19088199]
50. Denison MS, Pandini A, Nagy SR, Baldwin EP, Bonati L. Ligand binding and activation of the Ah receptor. Chem. Biol. Interact. 2002; 141:3–24. [PubMed: 12213382]

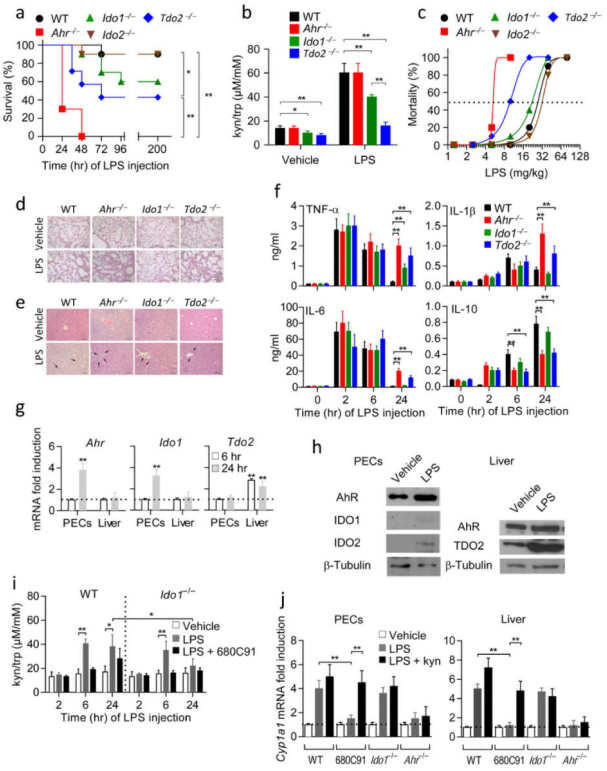

Figure 1. Increased susceptibility of *Tdo2*$^{-/-}$ and *Ahr*$^{-/-}$ mice to primary LPS challenge

a, Survival data of challenged mice (n = 10). One of three experiments. *P < 0.05; **P < 0.001 (log-rank test). **b**, Kyn/trp ratios. Mean ± s.d. of three experiments. *P < 0.05; **P < 0.001 (two-tailed Student's t-test). **c**, Estimation of LD_{50} (n = 10). **d,e**, Histopathology in lungs and liver, respectively. Scale bar, 100 μm. **f**, Cytokine measurements (means ± s.d.) from three experiments (n = 6; **P < 0.001; two-tailed Student's t-test). **g**, Gene transcript expressions. Means ± s.d. (three experiments; **P < 0.001; Shapiro test). **h**, Immunoblotting data. One experiment of three. **i**, Kyn/trp ratios (means ± s.d. of three experiments). *P < 0.05; **P < 0.001 (two-tailed Student's t-test). **j**, *Cyp1a1* transcript expression; three experiments; **P < 0.001 (Shapiro test).

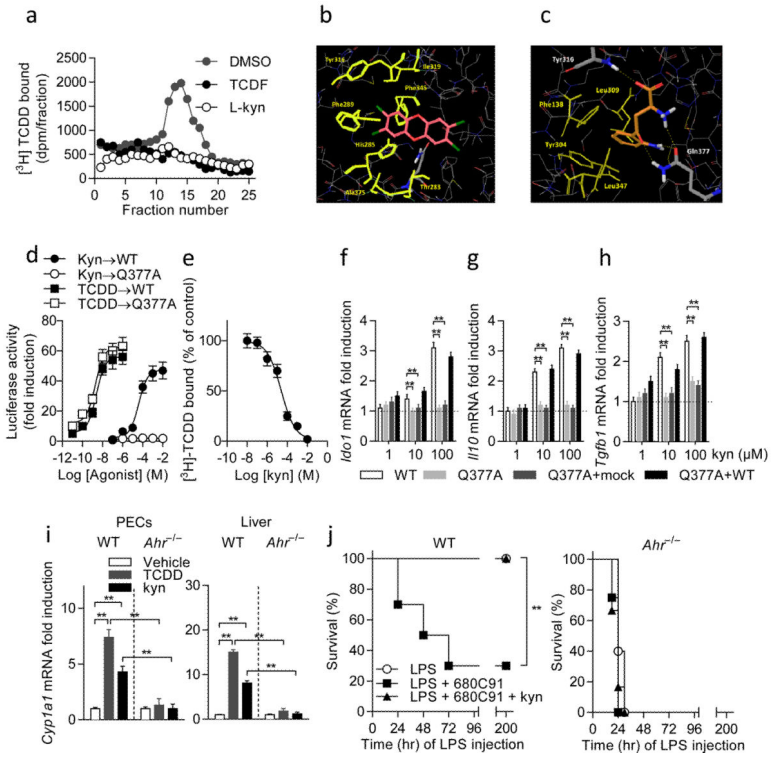

Figure 2. L-kynurenine (kyn) is an endogenous AhR ligand

a, Kyn competes with [^{3}H]TCDD for binding cytosolic AhR. **b,** Proposed binding mode of TCDD into the homology model of PAS-B of AhR. **c**, Proposed binding mode of kyn (orange carbon atoms) into the homology model of PAS-B of AhR. Hydrophobic residues involved in the binding of kyn are shown as yellow sticks. Gln377 is shown in sticks with carbon atoms in gray. **d**, Transactivation activity of WT or G377A AhR by kyn or TCDD. **e,** Competition by kyn for specific binding of [^{3}H]TCDD to cytosolic AhR from reconstituted *Ahr*$^{-/-}$ DCs, allowing for an estimated kyn IC_{50} value of 36.2 μM and of 21.6 μM for K_i. n = 3; means ± s.d. in one experiment of three. **f–h**, *Ido1*, *Il10* and *Tgfb1* transcripts. Means ± s.d. of three experiments; ** $P < 0.001$ (Shapiro test). **i**, *Cyp1a1* transcripts. Compiled data (means ± s.d.) from three experiments. **$P < 0.001$ (Shapiro test). **j**, Survival curves of variously treated mice (n = 10; one of three experiments). **$P < 0.001$ (log-rank test).

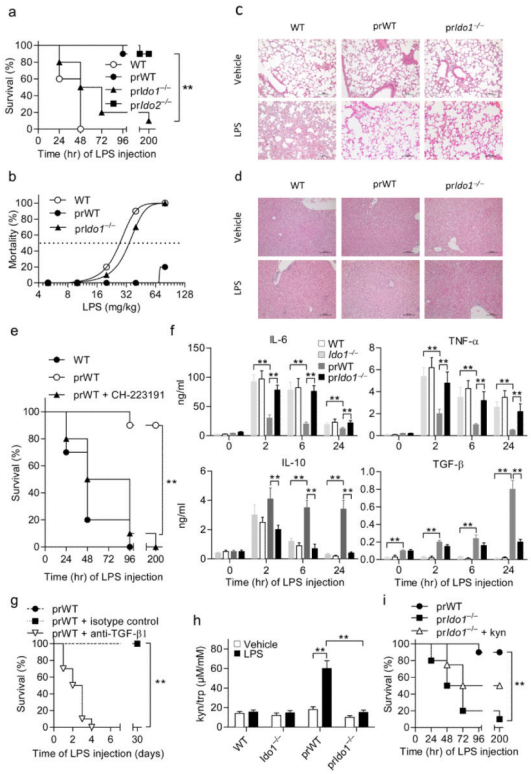

Figure 3. Absolute requirement for AhR, functional IDO1 and TGF-β in LPS tolerance

a, Survival of WT and LPS-primed WT (prWT), IDO1-deficient (pr*Ido1*$^{-/-}$) and TDO2-deficient (pr*Ido2*$^{-/-}$) mice after rechallenge. n = 8–10; one experiment of three. **P < 0.001; log-rank test. **b**, Endotoxin LD_{50} in tolerized mice. n = 10. **c,d**, Histopathology in lungs and liver, respectively; scale bar, 100 μm. One experiment of two. **e**, Survival of variously treated mice (n = 10; one of three experiments). **P < 0.001 (log-rank test). **f**, Cytokine measurements (mean ± s.d. of three experiments; n = 6). **P < 0.001 (two-tailed Student's t-test). **g**, Neutralization of TGF-β upon LPS rechallenge (n = 10). Three experiments (mean ± s.d.); **P < 0.001 (log-rank test). **h**, Kyn/trp ratios (mean ± s.d. of three experiments). **P < 0.001 (two-tailed Student's t-test). **i,** Survival of variously treated mice. n = 8–10; one experiment of three. **P < 0.001 (log-rank test).

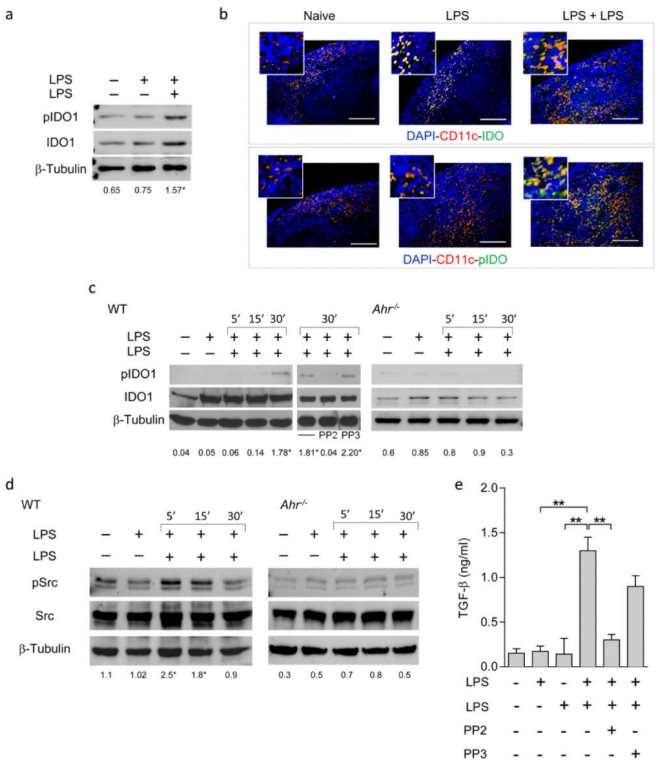

Figure 4. LPS tolerance induces AhR- and Src-dependent IDO1 phosphorylation

a, Phosphorylation of IDO1 in total splenocytes isolated from LPS-tolerant mice in one experiment of three. Ratios are mean values from the three experiments. *$P < 0.001$ (15' *vs.* single LPS exposure; two-tailed Student's *t*-test). **b**, Splenic immunofluorescent staining. Scale bar, 100 μm. **c**, Phosphorylation of IDO1's ITIM2 in WT and AhR-deficient cDCs. One experiment of three, ratios being means from the three experiments. *$P < 0.001$ (30' *vs.* single LPS exposure; two-tailed Student's *t*-test). **d**, Immunoblot analysis of Src and phosphorylated Src-Y416 (pSrc) in WT and AhR-deficient cDCs in one experiment of three. Ratios are means of the three experiments. *$P < 0.001$ (5' and 15' *vs.* single LPS exposure; two-tailed Student's *t*-test). **e**, Production of TGF-β by Src-competent cDCs in response to single or double LPS exposure. Means ± s.d. from three experiments; **$P < 0.001$ (two-tailed Student's *t*-test).

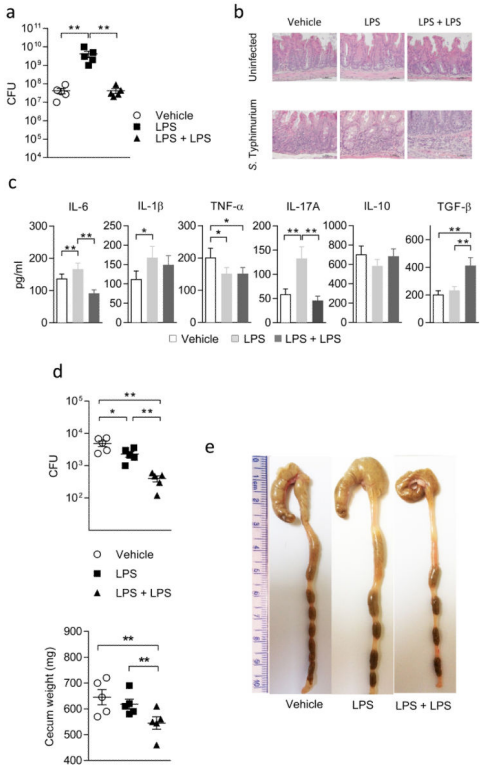

Figure 5. LPS tolerance ameliorates *S*. Typhimurium infection

a, Mice, treated once or twice with LPS, were challenged with *S.* Typhimurium, and bacterial counts assessed in cecum (CFU); $^{**}P < 0.001$; two-tailed Student's *t*-test; **b**, H&E staining of cecal tissues; **c**, cytokines in cecum cell supernatants. Data are means (± s.d.) from three experiments; $^{*}P < 0.05$, $^{**}P < 0.01$; two-tailed Student's *t*-test. **d**, Cecal CFU and cecal weights at 14 days post infection in tolerant mice. Three experiments; means ± s.d., with $^{*}P < 0.05$ and $^{**}P < 0.001$; two-tailed Student's *t*-test. **e**, Gross histopathology of cecum and distal colon (1 cm ruler scale).

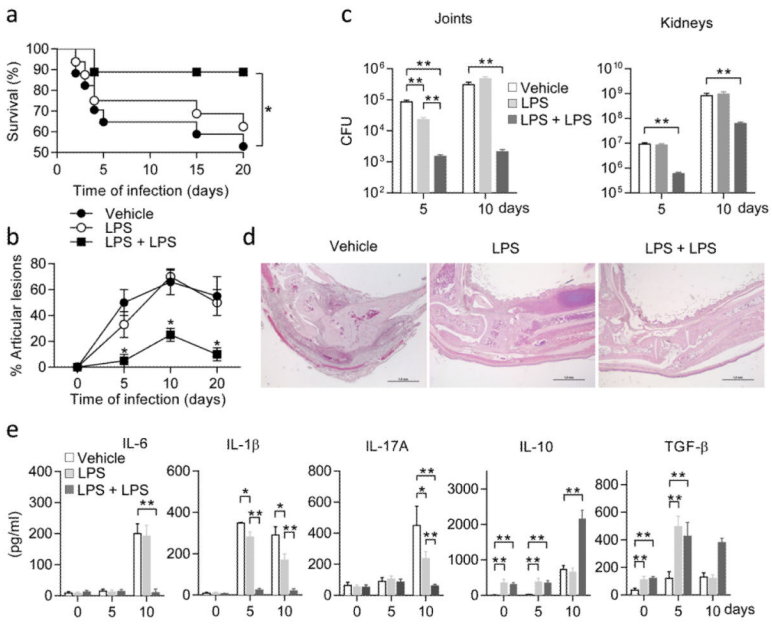

Figure 6. LPS tolerance protects against *Streptococcus* immunopathology

a, Survival of variously treated, infected mice (**P* < 0.05; log-rank test). **b**, Arthritis index. **c**, CFU enumeration in joints and kidneys. In **b** and **c,** values are means ± s.d. of three experiments; **P* < 0.05 and ***P* < 0.001; two-tailed Student's *t*-test. **d**, Histopathologic evaluation of arthritis in joints from LPS-tolerant, GBS-infected mice. Representative data from one of three experiments. Scale bar, 1mm. (**e**) Supernatants from joint homogenates were assayed kinetically for IL-6, IL-1β, IL-17A, IL-10, and TGF-β content. Values are the mean ± s.d. of three experiments. **P* < 0.05 and ***P* < 0.001, two-tailed Student's *t*-test.